



Experimental study on the reduction of sludge by a process of the synergistic effect of swirl cutting and ozone oxidation

Bo Zhang^{a,b,c}, Pengfei Ni^a, Xin Pu^a, Xiaohong Xu^{a,b,*}, Chundu Wu^{a,c}

^aSchool of the Environment and Safety Engineering, Jiangsu University, Zhenjiang 212013, China, emails: xuxiaohong@yeah.net (X. Xu), tabol@126.com (B. Zhang), 2420283291@qq.com (P. Ni), ozonemetal@126.com (X. Pu), wucd@ujs.edu.cn (C. Wu)

^bChangzhou Engineering and Technology Institute of Jiangsu University, Changzhou 213164, China

^cJiangsu Collaborative Innovation Center of Technology and Material of Water Treatment, Suzhou 215009, China

Received 27 March 2023; Accepted 28 July 2023

ABSTRACT

The residual sludge in the secondary sedimentation tank of the municipal sewage treatment plant was taken as the treatment object, the synergistic effect of swirl cutting and ozone oxidation was used to investigate the sludge reduction effect and the effect of the process on sludge lysis cells. The results showed that the mixed decomposition of sludge (swirl cutter and ozone treatment) was better than ozone alone. The removal rates of mixed liquor suspended solids and mixed liquor volatile suspended solids were 85.6% and 91%, respectively, when the ozone dosage rate was 15 mg·O₃·g⁻¹ suspended solids (SS). A better sludge reduction effect could be achieved with a lower ozone dosage rate. By examining microscope images with different magnifications before and after sludge treatment, it can be established that the swirl cutting process can disintegrate the sludge floc, thereby making the sludge floc into smaller particles and allowing ozone to be in full contact with the sludge floc. The carbon release effect of the sludge was characterized by chemical oxygen demand dissolution rate, which continued to increase with increasing ozone dosage. Total nitrogen (TN), total phosphorus (TP), PO₄³⁻-P, and polysaccharide leaching continued to grow with increasing ozone dosage, with the concentration of TN increasing from 2.83 to 33.27 mg·L⁻¹, 11.76 times the initial concentration. The concentration of TP increased from 5.2 to 13.14 mg·L⁻¹ at 15 mg·O₃·g⁻¹ SS, the concentration of PO₄³⁻-P increased from 3.75 to 12.8 mg·L⁻¹ and the concentration of polysaccharides increased from 7 to 37 mg·L⁻¹. Three-dimensional fluorescence was used to look at the changes in dissolved organic matter in the liquid phase of sludge both before and after treatment. The synergistic effects of swirl cutting and ozone oxidation resulted in the oxidation and decomposition of fulvic acid and aromatic protein I into small molecules without fluorescent characteristics.

Keywords: Swirl cutting; Sludge reduction; Lysis cells; Release intercellular material; Ozone

1. Introduction

Sewage sludge (wastewater treatment solids) is a rich source of nutrients and organic material [1]. The generation of excess sludge has increased recently as a result of the adoption of activated sludge techniques in numerous wastewater treatment plants. If this excess sludge is not properly treated and disposed of, it will seriously harm the environment

and natural resources [2]. However, traditional methods of sludge disposal and treatment are often constrained by their adverse environmental impacts, large footprints, and high costs. Therefore, treating sludge at the source is considered the most direct and effective strategy to solve these problems [3]. Under the current circumstances of excessive sludge production, limited alternatives of disposal, and high treatment and disposal costs, the development of sludge reduction technologies has emerged as one of the most important

* Corresponding author.

approach to address the sludge problem. The three types of such sludge reduction technologies include predation, metabolic decoupling, and stealth growth. One of these technologies has good potential based on cryptic growth, which is the anabolic use of cell lysis products by microorganisms. The sludge cells dissolve and release intracellular material after being treated with lysis cells, and the treated sludge is then added back to the biochemical tank as a secondary substrate to encourage the cryptic growth of other microbes, thereby lowering sludge formation. Lysis-cryptic growth can further be improved by several techniques including alkaline [4], Fenton [5], ultrasonic, ozone, etc. Ozonation is a promising method of reducing excess sludge in wastewater treatment plants [6], and ozone oxidation technology has been applied for the sludge reduction in municipal wastewater treatment plants. Ozone reacts with sludge mainly by breaking the sludge cells through its strong oxidizing properties. It causes the sludge cells to lyse and release the intracellular substances by oxidizing and decomposing the leached intracellular macromolecular organic matter into smaller molecules. However, practically ozone and sludge reactions are ineffective in terms of mass transfer. As sludge problems have become more severe, further research is being conducted to enhance ozone sludge reduction technology and its integration with other technologies. Yasui et al. [7,8] attained zero sludge discharge in the 1990s via the use of ozone to reduce residual sludge. Qiang et al. [9] achieved a maximum sludge reduction efficiency of 85% for 141 d of continuous operation of a pilot-scale treatment system combining sludge ozonation with the A²/O process. Huang et al. [10] proposed an *in-situ* sludge reduction process based on Mn²⁺ catalyzed ozone conditioning. This study offers a synergistic effect of swirl cutting and ozone oxidation to investigate the effect on sludge reduction, carbon source release, and sludge lysis cells based on the current trends of ozone oxidation sludge reduction technology.

2. Material and methods

2.1. Experimental sludge

Sludge from a secondary settling tank in the A²/O process of a sewage treatment facility was obtained for the experimentations, transported back to the lab, and mixed with tap water to bring the sludge concentration to around 4 g·L⁻¹. Specific sludge indicators are shown in Table 1. In the experiment, the sludge reduction effect was characterized by the

Table 1
Initial index of sludge in the test group

Indicators	Test sludge
MLSS (mg·L ⁻¹)	3,950
MLVSS (mg·L ⁻¹)	1,230
MLVSS/MLSS	0.31
Supernatant COD (mg·L ⁻¹)	47.62
Supernatant TP (mg·L ⁻¹)	5.2
Supernatant ammonia nitrogen (mg·L ⁻¹)	1.232
pH	9

removal rates of mixed liquor suspended solids (MLSS) and mixed liquor volatile suspended solids (MLVSS) instead of suspended solids (SS) and volatile suspended solids. MLSS is generally used in biological ponds and characterizes the sludge concentration of the biological system. SS refer to the suspended solids contained in the inlet and outlet, with many pollutants, including chemical oxygen demand (COD), P, etc., which is a kind of influent water quality parameter. MLVSS indicates the concentration of organic solids in activated sludge, which better reflects sludge activity.

Other meanings of indicators: (supernatant COD refers to the concentration of chemical oxygen demand in the supernatant. Supernatant TP denotes the concentration of total phosphorus in the supernatant. Supernatant ammonia nitrogen is the concentration of ammonia nitrogen in the supernatant. (Supernatant is defined as the cleaner liquid that is above the sludge after changing the sludge to water ratio and letting it sit for a while).

2.2. Swirl cutter

The swirl cutter is shown in Fig. 1. Parameters: internal diameter: 48 mm, ozone inlet diameter: 6 mm, pipe outlet diameter: 10 mm.

2.3. Experimental setup and methods

Sludge from the sludge reactor is pumped through the pipe into the swirl cutter and then flows back into the sludge reactor. In this process, firstly sludge enters the swirl chamber where swirl cutter rotates at high-speed forming a swirl conditions resulting in a reduction in pressure at the center of the swirl. When this pressure is below the saturation vapor pressure of the liquid, swirl cutting occurs, and the cutting bubbles are ejected from the outlet of the swirl cutter with the sludge. When normal pressure is restored in the sludge reactor, the cutting bubbles are collapsed. The collapse of the cutting bubbles generates strong shear and penetration forces in the fluid, hence destroying sludge flocs and cell walls. While the cutting cleaves hydroxyl radicals formed by the water molecules, which can trigger a strong redox reaction, destroying sludge flocs, dissolving cells and releasing intracellular substances [11], oxidizing the dissolved organic matter to carbon dioxide and water for sludge minimization [12]. On the other hand, the ozone generated by ozone generator through industrial oxygen, enters the swirl cutter. The swirl shears it into ozone microbubbles, which flow out and react with the sludge in the sludge reactor to improve the mass transfer of ozone. During the sludge treatment process, the sludge is continuously pumped through the swirl cutter, allowing it to be recycled into the sludge reactor.

The sludge was dosed at a volume of 30 L and the pH was adjusted to 9. The ozone concentration used was 60 mg·L⁻¹, the ozone gas flow rate was 1 L·min⁻¹, and the total ozone dose was 15 mg·O₃·g⁻¹ SS. The sludge flow rate was 14 L·min⁻¹, and the sludge line pressure was 0.4 MPa.

2.4. Analysis methods

The concentrations of COD, TP, ammonia nitrogen (NH₄⁺-N), total nitrogen (TN), nitrate nitrogen (NO₃⁻-N), and

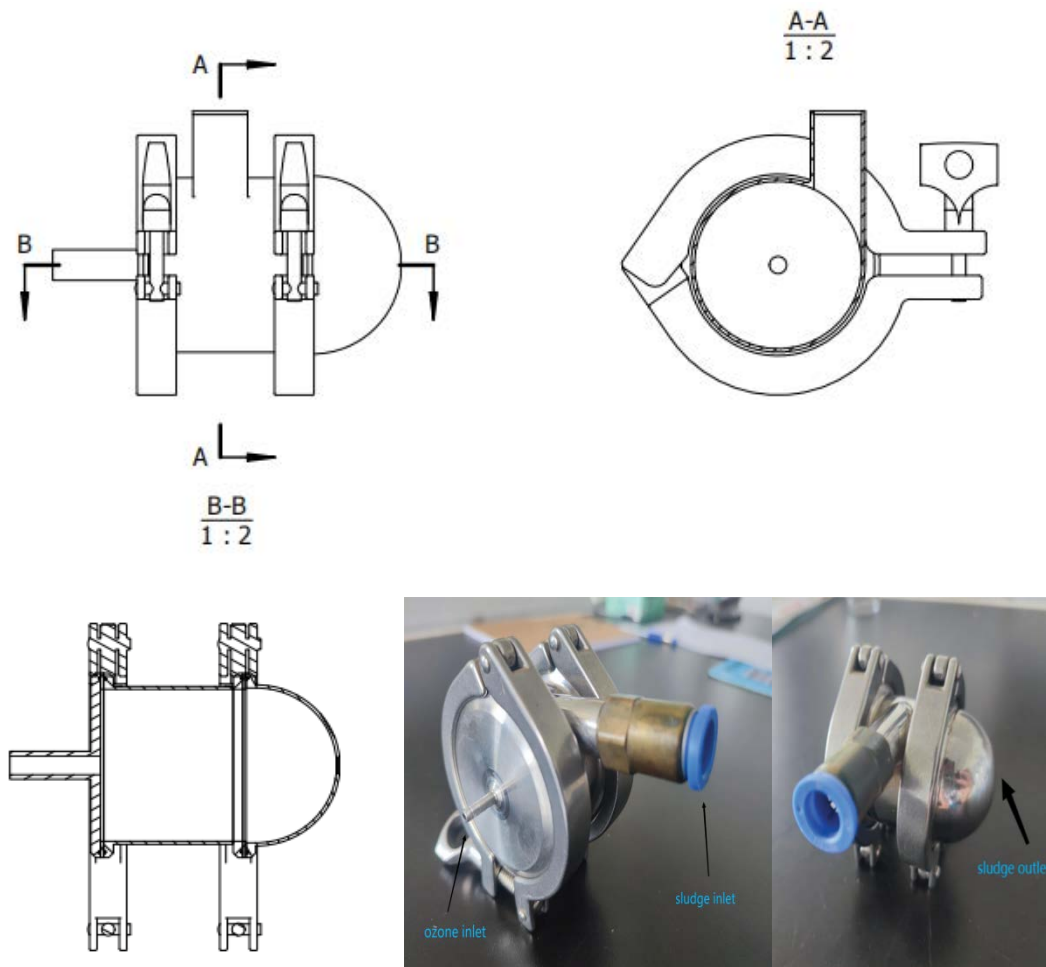


Fig. 1. Physical picture and CAD picture of swirl cutter.

nitrite nitrogen (NO_2^- -N) were determined by using Lianhua Technology's 5B-3B multi-parameter water quality analyzer. Concentrations of biochemical oxygen demand (BOD), and orthophosphate (PO_4^{3-} -P) were determined by using standard analytical methods. The concentration of organic nitrogen (ON) was the difference between the concentrations of TN, NH_4^+ -N, NO_3^- -N, and NO_2^- -N. Protein was determined by using the Komax Brilliant Blue method and polysaccharides were determined by using the phenol-sulphuric acid method. The chemical oxygen demand dissolution rate (DD_{COD}) [13] provides a more intuitive characterization of the degree and rate of release of carbon sources from the sludge and was calculated as follows.

$$\text{DD}_{\text{COD}} = \frac{\text{SCOD}_t - \text{SCOD}_0}{\text{TCOD} - \text{SCOD}_0} \times 100\% \quad (1)$$

TCOD is the COD concentration of sludge mixture before treatment, $\text{mg}\cdot\text{L}^{-1}$; SCOD_0 is the COD concentration of sludge supernatant before treatment, $\text{mg}\cdot\text{L}^{-1}$; SCOD_t is the COD concentration of sludge supernatant at time t after treatment. The sludge reduction effect was characterized by the removal rates of MLSS and MLVSS.

$$\text{MLSS Removal Rate} = \frac{\text{MLSS}_0 - \text{MLSS}_t}{\text{MLSS}_0} \times 100\% \quad (2)$$

$$\text{MLVSS Removal Rate} = \frac{\text{MLVSS}_0 - \text{MLVSS}_t}{\text{MLVSS}_0} \times 100\% \quad (3)$$

The 3D fluorescence spectra of the sludge supernatant were measured using a Hitachi F-7000 3D fluorescence spectrophotometer. Test conditions: excitation wavelength (Ex) 200–500 nm at 5 nm intervals; emission wavelength (Em) 250–600 nm at 5 nm intervals; scanning speed $1,000 \text{ nm}\cdot\text{min}^{-1}$, excitation/emission slit 5 nm.

3. Results and discussion

3.1. Sludge reduction effect

To illustrate the benefit of the synergistic effect of swirl cutting and ozone oxidation, the effect of ozone action alone was compared with the effect of sludge reduction using the variations of MLSS and MLVSS. Figs. 3 and 4 display the MLSS and MLVSS sludge removal rates, respectively.

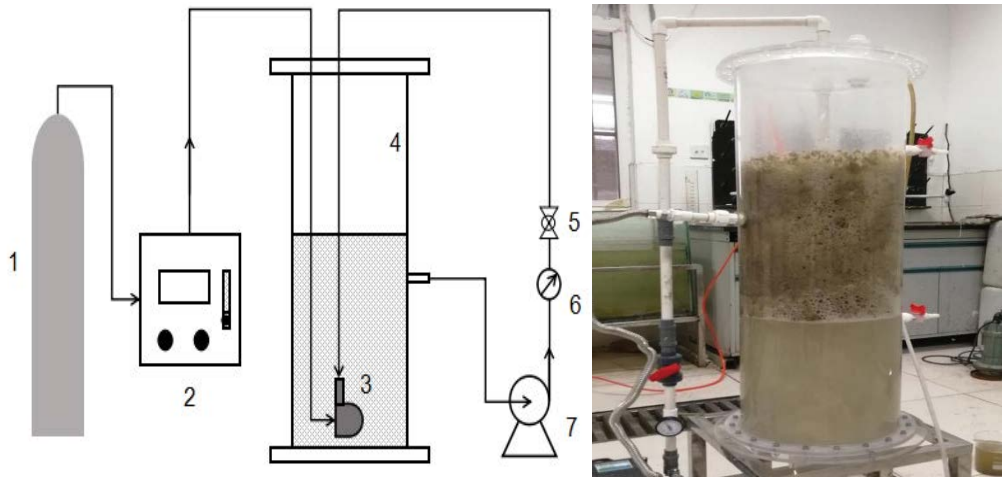


Fig. 2. Experimental apparatus (1) oxygen bottle; (2) ozone generator; (3) swirl cutter; (4) sludge reactor; (5) flowmeter; (6) pressure gauge; (7) water pump.

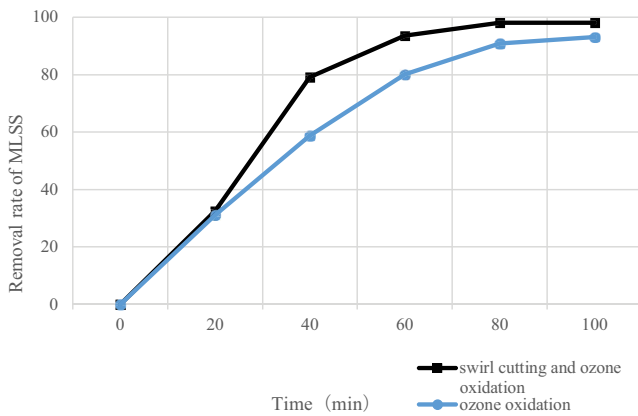


Fig. 3. Changes of MLSS removal rate under different treatment methods.

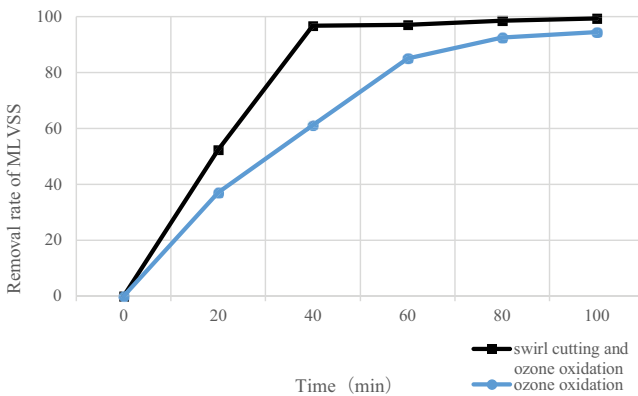


Fig. 4. Changes of MLVSS removal rate under different treatment methods.

From Fig. 3 it can be seen that the MLSS decreases rapidly and the MLSS removal rate is high due to the synergistic effect of swirl cutting and ozone oxidation; at 60 min, the MLSS removal rate reaches 93.6%, and by 80 min, it

approaches 98%. The rate of MLSS reduction in the ozone oxidation method was slightly slower than that in the synergistic effect of swirl cutting and the ozone oxidation method, and the MLSS removal rate reached 90.9% at 80 min, and then the MLSS remained basically unchanged, and the MLSS removal rate was 93.1% at 100 min. The variations of MLVSS and MLVSS removal rate are comparable to those of MLSS and MLSS removal rate, as shown in Fig. 4. The MLVSS decreases more quickly owing to the synergistic effect of swirl cutting and ozone oxidation than the ozone-oxidized sludge method. Due to the synergistic effects of swirl cutting and the ozone oxidation approach, the MLVSS removal rate increased to 96.7% at 40 min and then gradually reaches to 99.4% at 100 min. The MLVSS removal rate using the ozone oxidation approach was 92.6% at 80 min, and then it stayed essentially stable until it reached 94.5% at 100 min.

The sludge has a high rate of MLSS and MLVSS removal due to the synergistic impact of swirl cutting and ozone oxidation; the required reaction time is short; and the treatment efficiency is high. This demonstrates how the combined effects of swirl cutting and ozone oxidation can increase the effectiveness of reducing sludge.

To further investigate the reduction effect, we set the optimal ozone concentration. Fig. 5 illustrates the fluctuation in MLSS and MLVSS removal rates as well as the MLVSS and MLSS values of the sludge with ozone dosage under optimal process conditions.

The trends of the MLSS and MLVSS removal rates under different ozone dosages were compared. The MLVSS removal rates were greater than MLSS removal rates, it was noticed that the removal rates are faster prior to the ozone dose of $10 \text{ mg-O}_3\cdot\text{g}^{-1} \text{ SS}$ and they slightly slowdown after the ozone dosage of $10 \text{ mg-O}_3\cdot\text{g}^{-1} \text{ SS}$. The removal rates of MLSS and MLVSS were 85.6% and 91%, respectively, at an ozone dose of $15 \text{ mg-O}_3\cdot\text{g}^{-1} \text{ SS}$, and the MLVSS/MLSS value decreased from the initial 0.32 to 0.18. It can be seen that with the synergistic effect of swirl cutting and ozone oxidation, a better sludge reduction can be achieved with a lower ozone dosage. This is because the large specific surface area of ozone microbubbles improves the gas-liquid

mass transfer efficiency of ozone, which is conducive to the adequate reaction between ozone and sludge. MLVSS is a part of MLSS, and MLVSS/MLSS decreases mainly because sludge lysis is the most important factor. MLSS decreases mainly because organic matter in sludge particles dissolves into the liquid phase with the rupture of cell walls and cell membranes after sludge lysis, resulting in a rapid decrease in organic matter in the solid phase of sludge. The sludge MLVSS/MLSS values decreased significantly faster after the ozone dosage of $10 \text{ mg-O}_3\cdot\text{g}^{-1} \text{ SS}$, while the removal rate of MLSS and MLVSS increased faster before the ozone dosage of $10 \text{ mg-O}_3\cdot\text{g}^{-1} \text{ SS}$. This indicates that the reaction between swirl cutting and synergistic ozone oxidation was dominated by lysis in the early stage and mineralization in

the later stage. In the later stage of the reaction, the mineralization of organic matter was greatly enhanced by the synergistic effect of ozone and swirl cutting.

3.2. Sludge floc structure

The sludge floc may be destroyed during the swirl cutting operation, breaking it up into smaller pieces. Fig. 6 displays microscopic images of treated and untreated sludge at different magnifications. The cracking mechanism of sludge can be further analyzed using these images.

Before treatment, the sludge structure was seen to be tight, bulky, and clumped together, and the sludge cells were found to contain a significant amount of chemicals (40×16 times). The sludge grew thinner after treatment, and the sludge flocs were broken and no longer in obvious clumps. It is evident that swirl cutting has the ability to break up and disperse sludge flocs into smaller particles. Ozone can fully interact with the sludge floc in this manner.

3.3. Carbon source release effect

The residual sludge contains a large amount of carbon material, which is released into the sludge supernatant after sludge lysis cells and can be used as a carbon source back to be decomposed and utilized by other microorganisms. The variation of SCOD and BOD with ozone dosage during the sludge reduction process is shown in Fig. 7.

The supernatant's SCOD and BOD revealed an overall tendency to rise with increasing ozone dosage. With an ozone dose of $15 \text{ mg-O}_3\cdot\text{g}^{-1} \text{ SS}$, the SCOD increased from 47.62 to 360.5 mg-L^{-1} , which is 7.57 times greater than the initial concentration, while BOD increased from 8.7 to 113.2 mg-L^{-1} , which is 13.01 times higher than the initial concentration.

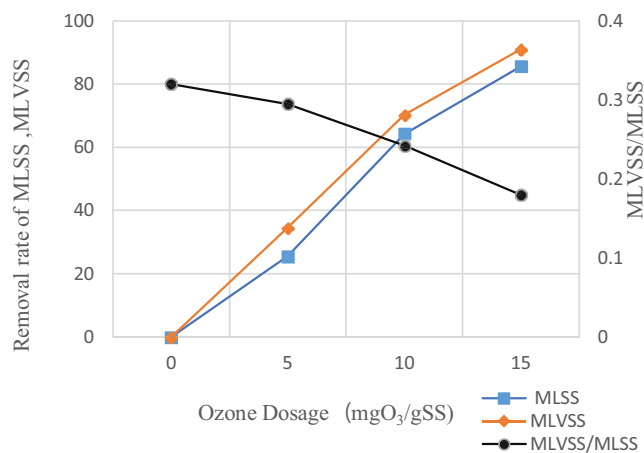


Fig. 5. Changes in MLSS and MLVSS removal rate and MLVSS/MLSS with ozone dosage.

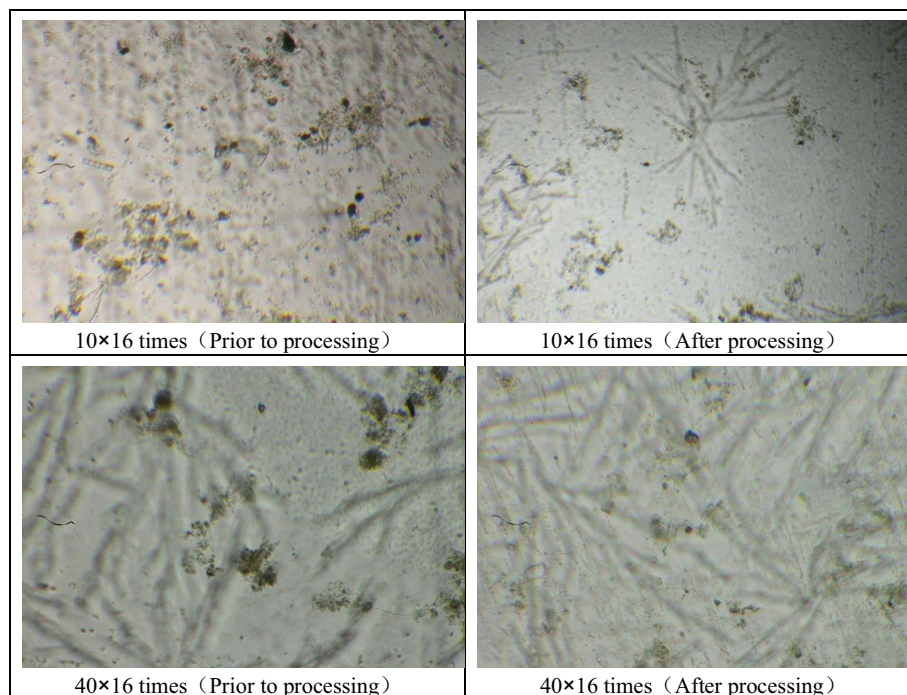


Fig. 6. Microscope images at different magnifications before and after sludge treatment.

Prior to the ozone dose of $5 \text{ mg}\cdot\text{O}_3\cdot\text{g}^{-1}$ SS and after the ozone dose of $5 \text{ mg}\cdot\text{O}_3\cdot\text{g}^{-1}$ SS, the added value of SCOD and BOD in the supernatant were higher. The reason being that at the onset of the reaction, the process of the synergistic effect of swirl cutting and ozone oxidation was mainly to break the wall lysis cell, and a large amount of organic matter from the cell entered the liquid phase, and SCOD and BOD in the supernatant increased rapidly. With the increase of organic matter in the liquid phase, the ozone synergistic swirl cutting effect reacts with sludge cells and also with organic matter dissolved in the liquid phase. Cell lysis is reduced on the one hand, and some of the organic matter dispersed in the liquid phase is oxidized and degraded into tiny molecules or directly mineralized on the other hand, resulting in a decrease in the increment of SCOD and BOD.

The biochemical properties of the supernatant were characterized by B/C, which varied as shown in Fig. 8. With increasing ozone dosage, B/C showed a trend of increasing and decreasing simultaneously. At an ozone dosage of $5 \text{ mg}\cdot\text{O}_3\cdot\text{g}^{-1}$ SS, B/C increased from 0.18 to 0.35, and biochemical properties were significantly improved. At ozone dosages of $10 \text{ mg}\cdot\text{O}_3\cdot\text{g}^{-1}$ SS and $15 \text{ mg}\cdot\text{O}_3\cdot\text{g}^{-1}$ SS, B/C was decreased to 0.3 and 0.31, respectively. This is due to the BOD being partially oxidized and degraded by the synergistic effect of swirl cutting and ozone.

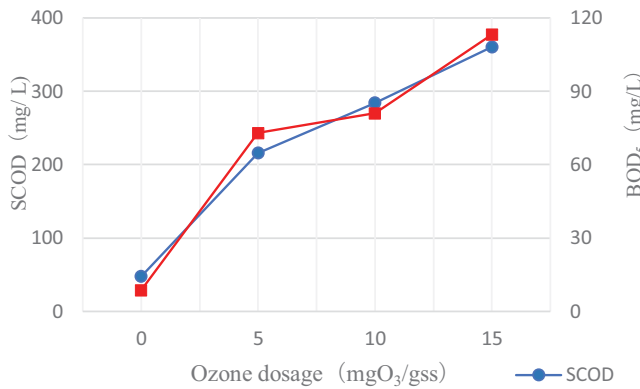


Fig. 7. Changes of SCOD and BOD in sludge supernatant with the dosage of ozone.

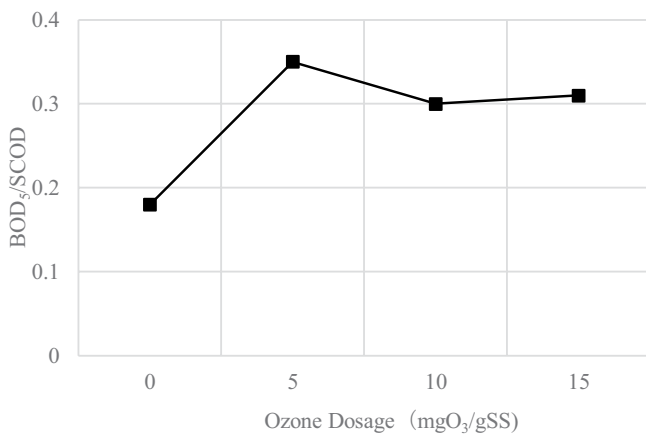


Fig. 8. Changes of B/C in sludge supernatant with ozone dosage.

DD_{COD} is a measure of the effect of carbon release from sludge. The fluctuation of TCOD and DD_{COD} with ozone dosage is shown in Fig. 9. As ozone exposure increases, TCOD falls and DD_{COD} rises. When the ozone dosage was $15 \text{ mg}\cdot\text{O}_3\cdot\text{g}^{-1}$ SS, DD_{COD} was 13.7%. DD_{COD} was not high primarily due to the fact that the ($-\text{OH}$) reaction predominated the ozone reaction under weak alkaline circumstances, whereas swirl cutting improved the oxidation efficiency of the ozone and synergistically produced a large amount of ($-\text{OH}$) with a strong mineralizing effect. It can be seen that the TCOD decreased continuously with increasing ozone dosage, from 2,323 to 630 $\text{mg}\cdot\text{L}^{-1}$, indicating that a large amount of organic matter was reacted and mineralized.

3.4. Release of elemental nitrogen

The variation of the content of each form of nitrogen in the sludge supernatant with the amount of ozone dosage is shown in Fig. 10.

With increasing ozone dosage, total nitrogen (TN) leaching continued to increase, with TN increasing from 2.83 to 33.27 $\text{mg}\cdot\text{L}^{-1}$ at an ozone dosage rate of $15 \text{ mg}\cdot\text{O}_3\cdot\text{g}^{-1}$ SS,

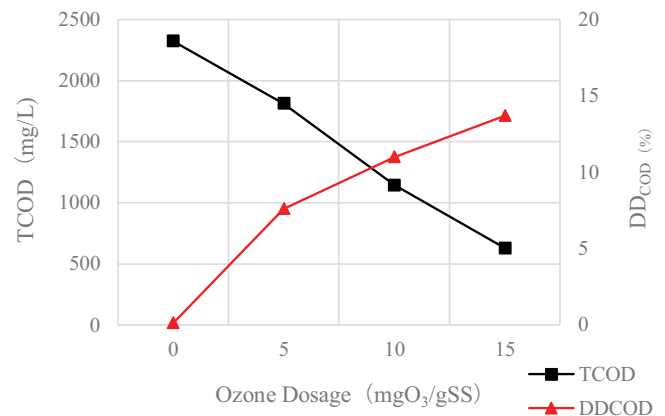


Fig. 9. Sludge TCOD, DD_{COD} variation with ozone dosage.

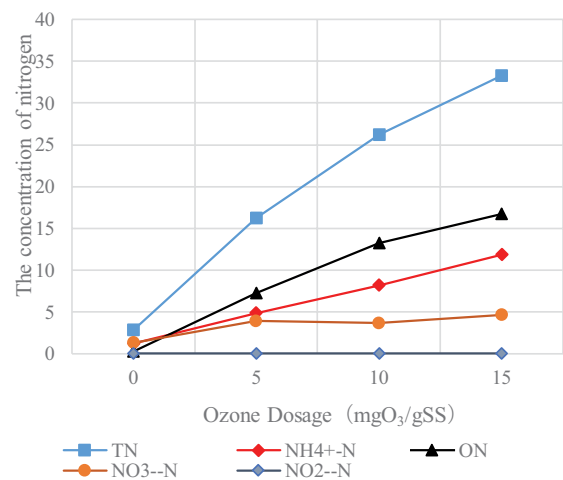


Fig. 10. Variation of nitrogen in the sludge supernatant with the amount of ozone dosage in each form.

11.76 times higher than the initial concentration. The significant increase in TN concentration in the liquid phase was mainly due to the rupture of sludge cells under the synergistic effect of ozone and swirl cutting, resulting in leaching of intracellular material and the transfer of large amounts of nitrogenous organic and inorganic substances from the solid phase to the liquid phase. As the reaction progresses, the rate of increase in TN slows down, indicating that sludge concentration and cellular leachable are decreasing, while the synergistic effect of swirl cutting and ozone oxidation begin to shift towards mineralization of the leached material. Ammoniacal nitrogen ($\text{NH}_4^+\text{-N}$) was increased from 1.232 to 11.85 $\text{mg}\cdot\text{L}^{-1}$, which represent 35.62% of the leached TN. Organic nitrogen (ON) was increased from 0.271 to 16.725 $\text{mg}\cdot\text{L}^{-1}$, representing 50.27% of the leached TN. It can be seen that the leached TN from the sludge was dominated by $\text{NH}_4^+\text{-N}$ and ON, with most present in the form of ON. This is primarily because, following the sludge lysis cell, a significant amount of nitrogenous organic matter, including proteins, nucleic acids, and humic acids, was released into the supernatant, leading to a rise in ON concentration. The spin-cutting effect produced ozone and -OH , which could further mineralize organic nitrogen into inorganic nitrogen and cause structural damage to proteins, nucleic acids, and humic acids. This slowed the rate of ON rise in the later stages of the reaction. $\text{NH}_4^+\text{-N}$ continued to increase as a result of the release of intracellular components and the conversion of ON. $\text{NO}_3^-\text{-N}$ increased from 1.303 to 4.651 $\text{mg}\cdot\text{L}^{-1}$, accounting for 13.95% of the dissolved TN, which was a relatively small increase and was essentially stable after the ozone dose of 5 $\text{mg}\cdot\text{O}_3\cdot\text{g}^{-1}$ SS, with a small increase. This is probably due to the fact that $\text{NO}_3^-\text{-N}$ originated mainly from the sludge floc, which initially adhered to the sludge surface and inside, and the sludge floc was broken up and $\text{NO}_3^-\text{-N}$ was released in the liquid phase without further change. The $\text{NO}_2^-\text{-N}$ concentration always remained at a lower level (<0.05 $\text{mg}\cdot\text{L}^{-1}$) and did not change much. This is mainly due to the low initial content of $\text{NO}_2^-\text{-N}$ and the ozone oxidation reaction degrades ammonia nitrogen in the water, so it is easily oxidized to $\text{NO}_3^-\text{-N}$ by the action of ozone [14].

3.5. Release of elemental phosphorus

The variation of TP and orthophosphate ($\text{PO}_4^{3-}\text{-P}$) leaching in the sludge supernatant with ozone dosage is shown in Fig. 11.

With increasing ozone dosage, the concentrations of TP and $\text{PO}_4^{3-}\text{-P}$ in the supernatant continued to increase, with TP increasing from 5.2 to 13.14 $\text{mg}\cdot\text{L}^{-1}$ and $\text{PO}_4^{3-}\text{-P}$ increasing from 3.75 to 12.8 $\text{mg}\cdot\text{L}^{-1}$ at an ozone dosage rate of 15 $\text{mg}\cdot\text{O}_3\cdot\text{g}^{-1}$ SS. The phosphorus in the sludge was mainly present in the sludge cell membranes and cytoplasm and was released from the sludge cells into the supernatant during the lysis process. The phosphorus was released from the sludge cells and into the supernatant. This shows that the combined action of swirl cutting and ozone oxidation damaged the sludge cell membranes. It can be seen that the TP in the supernatant is dominated by $\text{PO}_4^{3-}\text{-P}$, which can be recovered by adding guano stones first when the sludge is returned to the water to avoid an accumulation of phosphorus in the wastewater treatment system.

3.6. Polysaccharide release

The variation of polysaccharide concentration in the sludge supernatant is shown in Fig. 12.

Polysaccharides continued to increase as the ozone concentration rose, initially increasing more quickly and then gradually slowing down as time went on. The polysaccharide content increased from 7 to 37 $\text{mg}\cdot\text{L}^{-1}$, or 5.29 times the starting concentration, when the ozone dosage was 15 $\text{mg}\cdot\text{O}_3\cdot\text{g}^{-1}$ SS. Polysaccharides are a significant component of the extracellular polymer of sludge, as evidenced by their distribution and structural features. The extracellular sludge polymer was oxidized and destroyed in the liquid phase under the synergistic effect of swirl cutting and ozone oxidation, and the sludge lysis result was good, as revealed by the growth of polysaccharides in the sludge's liquid phase. Because the sludge substrate was reduced and some other polysaccharides that were dissolved in the liquid phase were oxidized and degraded into small molecules, the rate at which polysaccharides grew decreased as the reaction progressed.

3.7. Protein release

Protein contributes between 40% and 60% of the COD in the effluent, and Fig. 13 illustrates how the protein concentration in the sludge supernatant fluctuated. The protein

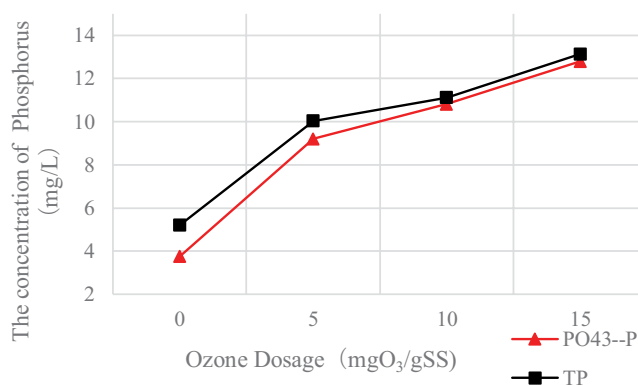


Fig. 11. Changes of TP and $\text{PO}_4^{3-}\text{-P}$ in sludge supernatant with the dosage of ozone.

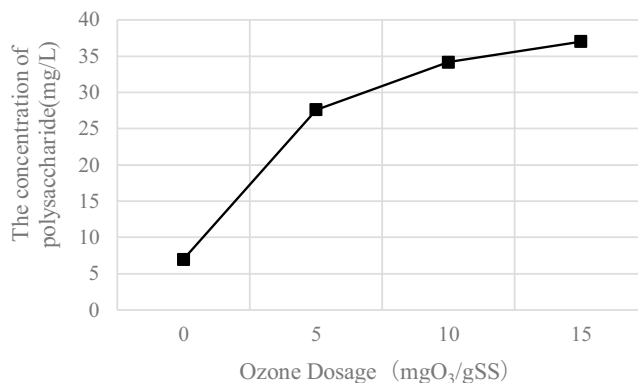


Fig. 12. Changes of polysaccharides in sludge supernatant with the dosage of ozone.

increased rapidly with increasing ozone concentration, and the rate of increase slowed down significantly after an ozone dosage rate of $10 \text{ mg}\cdot\text{O}_3\cdot\text{g}^{-1}$ SS. At an ozone dosage rate of $15 \text{ mg}\cdot\text{O}_3\cdot\text{g}^{-1}$ SS, the protein concentration increased from 3.06 to $8.41 \text{ mg}\cdot\text{L}^{-1}$, which was 2.75 times the initial concentration. This indicates that the sludge was well cytolyzed by the synergistic effect of ozone and swirl cutting, the intracellular material was dissolved and a large amount of protein material was released into the liquid phase. As the reaction progressed, the rate of protein increase slowed down. On the one hand, sludge concentration continued to decrease and cell soluble material decreased. On the other hand, under the weak alkaline conditions, ozone was mainly oxidized indirectly in the form of $-\text{OH}$, while the swirl cutting could enhance the oxidation efficiency of ozone, causing the protein structure to be destroyed and oxidized to small molecules of organic matter and ammonia nitrogen.

3.8. Three-dimensional fluorescence spectroscopy

The experimental mechanism was examined using three-dimensional fluorescence spectroscopy [15] based on the properties of the organic materials in the sludge supernatant. A lot of researchers have looked into the correlation between the dissolved organic matter (DOM's) fluorescence properties and the combined organic pollution indicators of wastewater. In wastewater, protein-like peaks predominate. Different DOM fluorescence areas in aquatic bodies have been categorized in numerous studies. Five

sections were separated into the 3D fluorescence spectrum, as shown in Table 2. The changes of organic compounds in the sludge supernatant before and after treatment were analyzed on the basis of fluorescence changes in the fluorescence spectrum region, and the action process of swirl cutting and ozone oxidation treatment on the sludge was further analyzed. The three-dimensional fluorescence spectrums of the sludge supernatant treatment before, and after the treatment process, and for the foam generation are shown in Figs. 14–16, respectively.

It can be seen from the fluorescence spectrums in Figs. 14–16 that before sludge treatment, the fluorescence peaks in zones II and IV were the most obvious, and zones I and III also had strong fluorescence intensity. The DOM in the sludge supernatant was dominated by aromatic proteins II and dissolved microbial metabolites, as well as some aromatic proteins I and fulvic acids. After sludge treatment, the fluorescence intensity of zone II and zone IV was significantly enhanced. After sludge treatment, cells were destroyed, sludge degradation was accelerated, and aromatic proteins II and microbial metabolites were the main organic matter dissolved in the cells. The fluorescence intensity of zone V was enhanced, and there was an obvious fluorescence peak. The sludge cells were destroyed, and a large number of humic acid substances in the sludge cells entered the sludge liquid phase. The fluorescence intensity of zone I and III decreased. Swirl cutting combined with ozone oxidation would not only destroy the sludge floc and lysate but

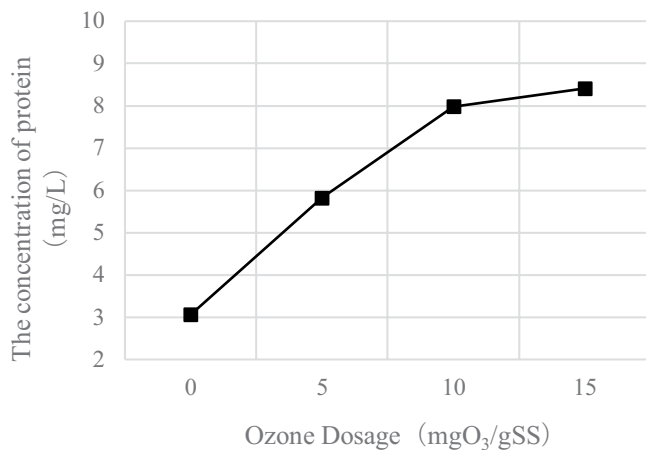


Fig. 13. Protein changes in sludge supernatant with ozone dosage.

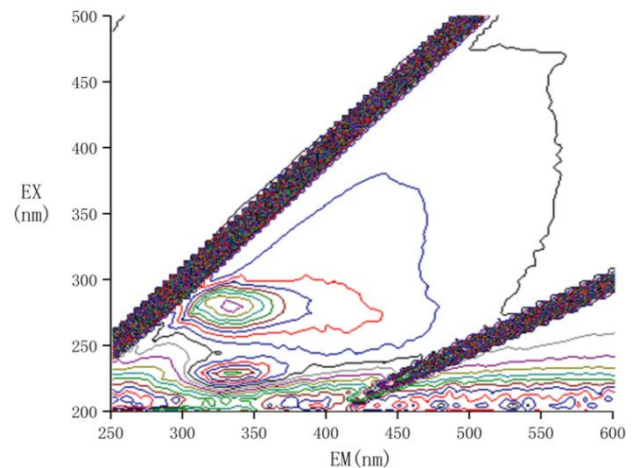


Fig. 14. Three-dimensional fluorescence spectrum of the sludge supernatant before treatment.

Table 2
Division of three-dimensional fluorescence spectrum region

Region number	Representing substance	Excitation wavelength (Ex)/nm	Emission wavelength (Em) /nm
I	Aromatic proteins I	200–250	250–330.
II	Aromatic proteins II	200–250	330–380.
III	Fulvic acids	200–250	>380
IV	Dissolved microbial metabolites	250–350	250–380.
V	Humic acids	250–500	>380

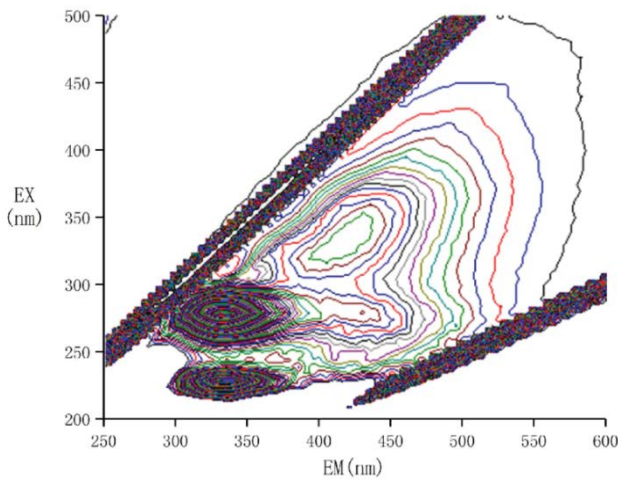


Fig. 15. Three-dimensional fluorescence spectrum of the sludge supernatant after treatment with ozone dosage of $15 \text{ mg} \cdot \text{O}_3 \cdot \text{g}^{-1} \text{ SS}$.

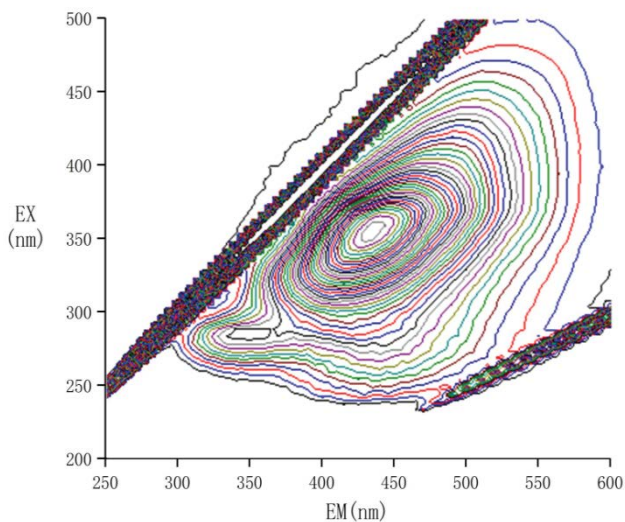


Fig. 16. Three-dimensional fluorescence spectra of foam generation with ozone dosage of $15 \text{ mg} \cdot \text{O}_3 \cdot \text{g}^{-1} \text{ SS}$.

also react with most of the aromatic proteins I and fulvic acids in the supernatant to degrade them into small molecules without fluorescence properties. By comparing the DOM in the supernatant before and after sludge treatment, it can be seen that the amount of organic matter in the supernatant increased. This increased content of organic matter was primarily composed of aromatic protein substances II and dissolved microbial metabolites, but it also contained a small amount of humic acid and fulvic acid substances, which speed up the decomposition of sludge and encouraged its return to the biochemical tank to be used by other microorganisms. In addition, the three-dimensional fluorescence map of the sludge foam shows that the fluorescence intensity of zone IV and zone V is very high, indicating that the DOM in the foam is mainly composed of dissolved microbial metabolites and humic acids. The fluorescence intensity of zone I, zone II and zone III was basically zero, that is,

there were no aromatic proteins I, aromatic proteins II and fulvic acids in the foam. By comparing the treated sludge supernatant and sludge foam, it can be seen that there are big differences in the composition of the two, which can be considered as being collected separately and used for different purposes or treatments.

4. Conclusion

Most sewage treatment plants adopt the activated sludge process. The treatment and disposal of a large amount of excess sludge has become a major problem in the water treatment industry. In this text, a process for sludge reduction by swirl cutting synergistic ozone oxidation treatment was proposed, and the sludge reduction effects of swirl cutting synergistic ozone oxidation treatment and ozone treatment alone were compared. The sludge characteristics and cell dissolution process of swirl cutting synergistic ozone oxidation sludge reduction were further investigated under optimal process conditions, and the mechanism of swirl cutting with ozone oxidation sludge reduction was briefly analyzed.

Under the swirl cutting synergistic ozone oxidation treatment, the sludge was treated with less ozone dose to achieve a better sludge reduction. According to the analysis of the removal rate of MLSS and MLVSS and the trend of MLVSS/MLSS value of the sludge, the swirl cutting synergistic ozone oxidation reacted with the sludge, with lysis dominating in the early stage and mineralization in the later stage. The carbon source of sludge was released more effectively. The SCOD increased from 47.62 to $360.5 \text{ mg} \cdot \text{L}^{-1}$, BOD increased from 8.7 to $113.2 \text{ mg} \cdot \text{L}^{-1}$, B/C increased from 0.18 to 0.31 and the supernatant biochemical properties were significantly improved. This is mainly due to the synergistic effect of swirl cutting and ozone on the sludge, which resulted in a large amount of intracellular organic matter entering the liquid phase from the solid phase, resulting in a rapid increase in SCOD and BOD in the supernatant.

The sludge supernatant continued to accumulate nitrogen and phosphorus under the swirl cutting with ozone oxidation treatment, and the total nitrogen (TN) increased from 2.83 to $33.27 \text{ mg} \cdot \text{L}^{-1}$, with $\text{NH}_4^+ \text{-N}$ and ON predominating. This shows that intracellular substances were leached out of the sludge as a result of the synergistic effect of swirl cutting and ozone, and a significant amount of nitrogenous organic and inorganic substances were transferred from the solid phase to the liquid phase, primarily proteins, nucleic acids, humic acids, and other nitrogenous organic matter. The TP increased from 5.2 to $13.14 \text{ mg} \cdot \text{L}^{-1}$, with $\text{PO}_4^{3-} \text{-P}$ dominating the TP. The increase in phosphorus in the supernatant indicates that the phosphorus in the supernatant increased, indicating that the sludge cell membranes were destroyed by the synergistic action of swirl cutting and ozone.

Three-dimensional fluorescence spectrum was used to further explore the changes of dissolved organic matter (DOM) in the sludge liquid phase before and after swirl cutting and ozone oxidation treatment. It was found that the DOM in the supernatant before sludge treatment was mainly composed of aromatic proteins II and dissolved microbial metabolites, and there were a small amount of aromatic proteins I and fulvic acids. After the swirl-current cutting and ozone oxidation treatments, the sludge cells were destroyed,

intracellular organic matter dissolved into the liquid phase, the aromatic proteins II and dissolved microbial metabolites in the supernatant increased, and a large number of humic acids appeared, while the aromatic proteins I and ferric acids in the supernatant reduced. It indicated that aromatic proteins I and fulvic acids were oxidized and decomposed into small molecules without fluorescence properties under the synergistic action of swirl cutting and ozone.

Acknowledgment

Thanks for the support of Jiangsu Water Conservancy Science and Technology Project (2021039) and Changzhou Sci&Tech Program (China, No.CJ20220025) on this study.

References

- [1] C.P. Del Río-Galván, R.C. Hernández-León, M.O. Franco-Hernández, J. Meléndez-Estrada, Primary sewage sludge treatment using a spiral support system, *Nat. Environ. Pollut. Technol.*, 21 (2022) 1167–1174.
- [2] X.H. Dai, Necessity and urgency of stabilization treatment of sewage sludge in urban wastewater treatment plant, *Water Waste Eng.*, 43 (2017) 12–13.
- [3] K.K. Xiao, Y. Chen, X. Jiang, Q. Yang, W.Y. Seow, W.Y. Zhu, Y. Zhou, Variations in physical, chemical and biological properties in relation to sludge dewaterability under Fe(II) - oxone conditioning, *Water Res.*, 109 (2017) 13–23.
- [4] Z.L. Jin, C.R. Cai, T. Hashimoto, Y.D. Yuan, D.H. Kang, J. Hunter, X.R. Zhou, Alkaline etching and desmutting of aluminium alloy: The behaviour of Mg₂Si particles, *J. Alloys Compd.*, 842 (2020) 17–19.
- [5] Z.Y. Yu, G.J. Zhao, H.W. Yu, Q. Liu, Z.Y. Zhang, R.F. Sun, W.G. Geng, L.Y. Wang, Iron-based denitration catalyst derived from Fenton sludge: optimization analysis of selective dealkalization and influence mechanism of calcination temperature, *J. Cleaner Prod.*, 378 (2022) 134524, doi: 10.1016/j.jclepro.2022.134524.
- [6] L. Wang, W.W. Ben, Y.G. Li, C. Liu, Z.M. Qiang, Behavior of tetracycline and macrolide antibiotics in activated sludge process and their subsequent removal during sludge reduction by ozone, *Chemosphere*, 206 (2018) 184–191.
- [7] H. Yasui, K. Nakamura, S. Sakuma, A full-scale operation of a novel activated sludge process without excess sludge production, *Water Sci. Technol.*, 96 (1996) 395–404.
- [8] H. Yasui, M. Shibata, An innovative approach to reduce excess sludge production in the activated sludge process, *Water Sci. Technol.*, 30 (1994) 11–20.
- [9] Z.M. Qiang, L. Wang, H.Y. Dong, J.H. Qu, Operation performance of an A/A/O process coupled with excess sludge ozonation and phosphorus recovery: a pilot-scale study, *Chem. Eng. J.*, 268 (2015) 162–169.
- [10] H.Z. Huang, T.T. Wei, H. Wang, B. Xue, S. Chen, X.K. Wang, H.B. Wu, B. Dong, Z.X. Xu, *In-situ* sludge reduction based on Mn²⁺-catalytic ozonation conditioning: feasibility study and microbial mechanisms, *J. Environ. Sci.*, 135 (2024) 185–197.
- [11] D.N.K. Vo, M. Tokuoka, N.T. Phan, V.Q. Tran, The effect of adding wood chips on the decomposition of sludge from seafood processing wastewater treatment system, *Earth Environ. Sci.*, 1009 (2022) 012003, doi: 10.1088/1755-1315/1009/1/012003.
- [12] R. Morello, F. Di Capua, G. Esposito, F. Pirozzi, U. Fratino, D. Spasiano, Sludge minimization in mainstream wastewater treatment: mechanisms, strategies, technologies, and current development, *J. Environ. Manage.*, 319 (2022) 115756, doi: 10.1016/j.jenvman.2022.115756.
- [13] M. Tokumura, H. Katoh, T. Katoh, H.T. Znad, Y. Kawase, Solubilization of excess sludge in activated sludge process using the solar photo-Fenton reaction, *J. Hazard. Mater.*, 162 (2009) 1390–1396.
- [14] Z.X. Yang, G.X. Yan, S.H. Guo, Electrocatalytic oxidation degradation of ammonia nitrogen wastewater, *J. Am. Chem. Soc.*, 257 (2019) 65–68.
- [15] E.S. Zhang, L.M. Wu, L. Jiang, K.F. Guo, Z.Y. Su, P. Ju, A novel amino functionalized three-dimensional fluorescent Zn-MOF: the synthesis, structure and applications in the fluorescent sensing of organic water pollutants, *J. Mol. Struct.*, 1264 (2022) 133314, doi: 10.1016/j.molstruc.2022.133314.